Simulation of Heisenberg *XY* interactions and realization of a perfect state transfer in spin chains using liquid nuclear magnetic resonance

Jingfu Zhang,[1,*] Gui Lu Long,[1,4,†] Wei Zhang,[2] Zhiwei Deng,[2,‡] Wenzhang Liu,[1] and Zhiheng Lu[3]
[1]*Key Laboratory For Quantum Information and Measurements of MOE, and Department of Physics, Tsinghua University, Beijing, 100084, China*
[2]*Testing and Analytical Center, Beijing Normal University, Beijing, 100875, China*
[3]*Department of Physics, Beijing Normal University, Beijing, 100875, China*
[4]*Key Laboratory For Atomic and Molecular Nanosciences, Tsinghua University, Beijing 100084, China*
(Received 4 April 2005; published 22 July 2005)

The three-spin chain with a Heisenberg *XY* interaction is simulated in a three-qubit nuclear magnetic resonance quantum computer. The evolution caused by the *XY* interaction is decomposed into a series of single-spin rotations and the *J*-coupling evolutions between the neighboring spins. The perfect state transfer algorithm proposed by Christandl *et al.*[Phys. Rev. Lett. **92**, 187902 (2004)] is realized in the *XY* chain.

DOI: 10.1103/PhysRevA.72.012331 PACS number(s): 03.67.Lx

I. INTRODUCTION

Quantum computers have great advantages over classical computers in solving some problems [1], such as simulating quantum systems [2], factorizing large numbers [3], and searching unsorted databases [4]. The theory of quantum networks has proved that single-qubit gates and two-qubit gates are universal for quantum computation [5].

There are several physical systems that can implement quantum computation [6]. Because of its technologic sophistication and convenience in manipulation, liquid NMR has been an important experimental method to implement quantum algorithms, demonstrate error-correcting codes, and simulate quantum systems [7]. Through liquid NMR one can learn lessons for building practical quantum computers in the future. The tools and techniques developed in liquid NMR, such as shaped pulses, pulse sequence simplification, and refocusing techniques, are widely used in other systems.

Interactions between qubits are necessary for quantum computation. Heisenberg interactions naturally exist in various spin systems and are expected to play important roles in building large-scale quantum computers [8]. In liquid NMR systems, the Heisenberg interaction exists in the form of *ZZ* interactions [9]; i.e., the interaction between two spins takes the form of $J_{mn}\sigma_z^m\sigma_z^n$ (*J* coupling in liquid NMR), where σ_z^m denotes the *z* component of the Pauli matrix for spin *m* and J_{mn} denotes the coupling constant between spins *m* and *n*. In the other systems, the Heisenberg interactions take more advanced forms. DiVincenzo *et al.* pointed out that the Heisenberg interaction alone can be universal for quantum computation if coded qubit states are introduced [10,11]. This result is exciting, because single-spin operations, which usually cause additional difficulties in manipulations in some systems, can be avoided. The perfect state transfer (PST) algorithm proposed by Christandl *et al.* satisfies such a condition that no single-spin operations are needed [12]. The algorithm can transfer an arbitrary quantum state between the two ends of a spin chain or a more complex spin network in a fixed period time only using *XY* interactions. If the state is transferred in a more than three-spin chain, the coded qubits are needed, so that the chain is extended to a network. Compared with the state transfer based on SWAP operations, where single-spin operations are used to switch on or off the couplings between spins [13], the PST algorithm is easy to implement in some solid systems.

In this paper, we simulate the Heisenberg *XY* interactions in a spin chain and realize the PST algorithm using a three-qubit liquid NMR quantum computer. In particular, the evolution caused by the *XY* interactions can be represented by single-spin operations and the *ZZ* interactions using a technique analogous to angular momentum algebra. Through this transformation, it is possible to simulate *XY* interactions using the liquid NMR system, although there are no real *XY* couplings in such a system.

II. SIMULATING THE THREE-SPIN *XY* CHAIN USING LIQUID NMR

The Hamiltonian for a three-spin *XY* chain with the neighboring Heisenberg interaction is

$$H_{XY}=\frac{1}{2}J(\sigma_x^1\sigma_x^2+\sigma_y^1\sigma_y^2+\sigma_x^2\sigma_x^3+\sigma_y^2\sigma_y^3), \tag{1}$$

where $\sigma_{x/y}^j$ $(j=1,2,3)$ are the Pauli matrices and *J* is the coupling constant between two spins. For convenience in expression, $\hbar$ has been set to 1. The evolution caused by H_{XY} can be expressed as

$$U(t)=e^{-iH_{XY}t}, \tag{2}$$

where *t* is the evolution time. In order to represent $U(t)$ in

*Electronic address: zhangjfu2000@yahoo.com
†Electronic address: gllong@mail.tsinghua.edu.cn
‡Electronic address: dengzw@bnu.edu.cn

 ©2005 The American Physical Society

liquid NMR version, we introduce two commutable operators $A=(\sigma_x^1\sigma_x^2+\sigma_y^2\sigma_y^3)/2$, and $B=(\sigma_y^1\sigma_y^2+\sigma_x^2\sigma_x^3)/2$. $U(t)$ can be rewritten as $U(t)=U_A(t)U_B(t)$, where

$$U_A(t)=e^{-iJtA}\equiv e^{-iJt(\sigma_x^1\sigma_x^2+\sigma_y^2\sigma_y^3)/2}, \tag{3}$$

$$U_B(t)=e^{-iJtB}\equiv e^{-iJt(\sigma_y^1\sigma_y^2+\sigma_x^2\sigma_x^3)/2}. \tag{4}$$

We define three operators $L_x^A\equiv\sigma_x^1\sigma_x^2/2$, $L_y^A\equiv\sigma_y^2\sigma_y^3/2$, and $L_z^A\equiv\sigma_x^1\sigma_z^2\sigma_y^3/2$. These operators can be viewed as the three components of the angular momentum vector denoted by L^A, because they satisfy the commuting conditions $[L_x^A,L_y^A]=iL_z^A$, $[L_y^A,L_z^A]=iL_x^A$, and $[L_z^A,L_x^A]=iL_y^A$. Equation (3) can be rewritten as

$$U_A(t)=e^{-iJt(L_x^A+L_y^A)}=e^{-i(\sqrt{2}Jt)L^A\cdot\mathbf{n}}, \tag{5}$$

where the vector $\mathbf{n}=(1/\sqrt{2},1/\sqrt{2},0)$, and it denotes the direction of the rotation axis for $U_A(t)$. The separate angles between $\mathbf{n}$ and x, y, and z axes are $\pi/4$, $\pi/4$, and $\pi/2$, respectively. Using the theories of angular momentum, we obtain

$$\begin{aligned}U_A(t)&=e^{-i(\pi/4)L_z^A}e^{-i\sqrt{2}JtL_x^A}e^{i(\pi/4)L_z^A}\\&=e^{-i(\pi/8)\sigma_x^1\sigma_z^2\sigma_y^3}e^{-i(Jt/\sqrt{2})\sigma_x^1\sigma_x^2}e^{i(\pi/8)\sigma_x^1\sigma_z^2\sigma_y^3}\\&=\cos\left(\frac{Jt}{\sqrt{2}}\right)I-\frac{i}{\sqrt{2}}\sin\left(\frac{Jt}{\sqrt{2}}\right)(\sigma_x^1\sigma_x^2+\sigma_y^2\sigma_y^3),\end{aligned} \tag{6}$$

where I denotes an identity operator.

In a similar way, through defining $L_x^B\equiv\sigma_x^2\sigma_x^3/2$, $L_y^B\equiv\sigma_y^1\sigma_y^2/2$, and $L_z^B\equiv\sigma_y^1\sigma_z^2\sigma_x^3/2$ as the three components of the angular momentum vector denoted as L^B, we obtain

$$\begin{aligned}U_B(t)&=e^{-i(\pi/4)L_z^B}e^{-i\sqrt{2}JtL_x^B}e^{i(\pi/4)L_z^B}\\&=e^{-i(\pi/8)\sigma_y^1\sigma_z^2\sigma_x^3}e^{-i(Jt/\sqrt{2})\sigma_x^2\sigma_x^3}e^{i(\pi/8)\sigma_y^1\sigma_z^2\sigma_x^3}\\&=\cos\left(\frac{Jt}{\sqrt{2}}\right)I-\frac{i}{\sqrt{2}}\sin\left(\frac{Jt}{\sqrt{2}}\right)(\sigma_y^1\sigma_y^2+\sigma_x^2\sigma_x^3).\end{aligned} \tag{7}$$

One can prove the last equations in Eqs. (6) and (7) directly through Eqs. (3) and (4) using $[(\sigma_x^1\sigma_x^2+\sigma_y^2\sigma_y^3)/\sqrt{2}]^2=1$ and $[(\sigma_y^1\sigma_y^2+\sigma_x^2\sigma_x^3)/\sqrt{2}]^2=1$. Combining Eqs. (6) and (7), we obtain

$$\begin{aligned}U(t)=&e^{-i(\pi/8)\sigma_x^1\sigma_z^2\sigma_y^3}e^{-i(Jt/\sqrt{2})\sigma_x^1\sigma_x^2}e^{i(\pi/8)\sigma_x^1\sigma_z^2\sigma_y^3}e^{-i(\pi/8)\sigma_y^1\sigma_z^2\sigma_x^3}\\&\times e^{-i(Jt/\sqrt{2})\sigma_x^2\sigma_x^3}e^{i(\pi/8)\sigma_y^1\sigma_z^2\sigma_x^3}.\end{aligned} \tag{8}$$

Each of the six factors in Eq. (8) can be realized using liquid NMR. Consequently the three-spin XY chain can be simulated in a three-spin liquid NMR system.

III. IMPLEMENTING THE PERFECT STATE TRANSFER ALGORITHM IN THE *XY* CHAIN

The PST algorithm was proposed by Christandl *et al.* [12], and it can be implemented in the XY chain. The algorithm can transfer an arbitrary quantum state between the two ends of the chain in a fixed period time, only using XY interactions. Unlike the state transfer based on SWAP operations [13], the PST algorithm does not require single-spin operations. Hence the algorithm is more feasible to realize in some systems, such as the electron-spin-resonance system, where single-spin operations cause many experimental difficulties [10].

Letting $\varphi\equiv Jt/\sqrt{2}$, Eq. (8) is represented as the matrix

$$U(t)=\begin{pmatrix}1&0&0&0&0&0&0&0\\0&\cos^2\varphi&-\frac{i}{\sqrt{2}}\sin(2\varphi)&0&-\sin^2\varphi&0&0&0\\0&-\frac{i}{\sqrt{2}}\sin(2\varphi)&\cos(2\varphi)&0&-\frac{i}{\sqrt{2}}\sin(2\varphi)&0&0&0\\0&0&0&\cos^2\varphi&0&-\frac{i}{\sqrt{2}}\sin(2\varphi)&-\sin^2\varphi&0\\0&-\sin^2\varphi&-\frac{i}{\sqrt{2}}\sin(2\varphi)&0&\cos^2\varphi&0&0&0\\0&0&0&-\frac{i}{\sqrt{2}}\sin(2\varphi)&0&\cos(2\varphi)&-\frac{i}{\sqrt{2}}\sin(2\varphi)&0\\0&0&0&-\sin^2\varphi&0&-\frac{i}{\sqrt{2}}\sin(2\varphi)&\cos^2\varphi&0\\0&0&0&0&0&0&0&1\end{pmatrix}. \tag{9}$$

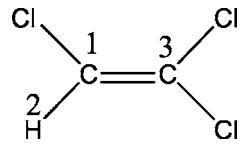

FIG. 1. The sketch of trichloroethylene (TCE). The three qubits are denoted as C1, H2, and C3, respectively.

The order of the basis states is $|000\rangle$, $|001\rangle$, $|010\rangle$, $|011\rangle$, $|100\rangle$, $|101\rangle$, $|110\rangle$, $|111\rangle$, where $|0\rangle$ and $|1\rangle$ denote the spin-up and -down states, respectively. When $t=\pi/\sqrt{2}J$, one obtains

$$U\left(\frac{\pi}{\sqrt{2}J}\right)=\begin{pmatrix}1&0&0&0&0&0&0&0\\0&0&0&0&-1&0&0&0\\0&0&-1&0&0&0&0&0\\0&0&0&0&0&0&-1&0\\0&-1&0&0&0&0&0&0\\0&0&0&0&0&-1&0&0\\0&0&0&-1&0&0&0&0\\0&0&0&0&0&0&0&1\end{pmatrix}. \tag{10}$$

Obviously, $U|000\rangle=|000\rangle$, $U|001\rangle=-|100\rangle$, $U|010\rangle=-|010\rangle$, $U|011\rangle=-|110\rangle$, $U|100\rangle=-|001\rangle$, $U|101\rangle=-|101\rangle$, $U|110\rangle=-|011\rangle$, and $U|111\rangle=|111\rangle$. We use $|\psi\rangle_{in}=(\alpha|0\rangle+\beta|1\rangle)|00\rangle$ as the input state by setting spin 1 into state $(\alpha|0\rangle+\beta|1\rangle)$, where α, β are two arbitrary complex numbers. $U(\pi/\sqrt{2}J)$ transforms $|\psi\rangle_{in}$ into $|00\rangle(\alpha|0\rangle-\beta|1\rangle)$, where spin 3 lies in state $(\alpha|0\rangle-\beta|1\rangle)$ and the perfect state transfer is completed.

The implementation of the PST algorithm in a two- or three-spin chain does not require coded qubits. However, in more than a three-spin chain, coded qubits are needed to come up with a design so as to extend the chain to a more complex network. The details can been found in [12].

IV. REALIZATION IN A THREE-QUBIT NMR QUANTUM COMPUTER

The experiments use a sample of carbon-13 labeled trichloroethylene (TCE) dissolved in d-chloroform. Data are taken with a Bruker DRX 500 MHz spectrometer. The temperature is controlled at 22 °C. The sketch of TCE is shown in Fig. 1. ^{1}H is denoted as qubit 2, the ^{13}C directly connecting to ^{1}H is denoted as qubit 1, and the other ^{13}C is denoted as qubit 3. The three qubits are denoted as C1, H2, and C3. T_1 is measured to be about 3.8 s, 4.7 s, and 4.2 s, and T_2 is measured to be about 0.40 s, 0.24 s, and 0.21 s, for C1, H2, and C3, respectively. The Hamiltonian of the three-qubit system is [14]

$$H_{NMR}=-\pi\nu_1\sigma_z^1-\pi\nu_2\sigma_z^2-\pi\nu_3\sigma_z^3+\frac{1}{2}\pi J_{12}\sigma_z^1\sigma_z^2+\frac{1}{2}\pi J_{23}\sigma_z^2\sigma_z^3+\frac{1}{2}\pi J_{13}\sigma_z^1\sigma_z^3, \tag{11}$$

where ν_1, ν_2, and ν_3 are the resonance frequencies of C1, H2, and C3. The center frequencies of C1 and C3 are 116.53 ppm and 123.76 ppm, respectively, and $\nu_3=\nu_1+909.2$ Hz. The coupling constants are measured to be $J_{12}=200.9$ Hz, $J_{23}=9.16$ Hz, and $J_{13}=103.1$ Hz. The coupled-spin evolution between two spins is denoted as

$$[\tau_{jl}]=e^{-i(1/2)\pi J_{jl}\tau\sigma_z^j\sigma_z^l}, \tag{12}$$

where $j/l=1,2,3$ and $j\neq l$. $[\tau_{jl}]$ can be realized by averaging the coupling constants other than J_{jl} to zero [15,16].

The three- and two-body interactions in Eq. (8) can be expressed as [17]

$$e^{-i(\pi/8)\sigma_x^1\sigma_z^2\sigma_y^3}=e^{-i(\pi/4)\sigma_y^1}e^{i(\pi/4)\sigma_x^3}e^{-i(\pi/8)\sigma_z^1\sigma_z^2\sigma_z^3}e^{i(\pi/4)\sigma_y^1}e^{-i(\pi/4)\sigma_x^3}, \tag{13}$$

$$e^{i(\pi/8)\sigma_x^1\sigma_z^2\sigma_y^3}=e^{-i(\pi/4)\sigma_y^1}e^{i(\pi/4)\sigma_x^3}e^{i(\pi/8)\sigma_z^1\sigma_z^2\sigma_z^3}e^{i(\pi/4)\sigma_y^1}e^{-i(\pi/4)\sigma_x^3}, \tag{14}$$

$$e^{-i(\pi/8)\sigma_y^1\sigma_z^2\sigma_x^3}=e^{i(\pi/4)\sigma_x^1}e^{-i(\pi/4)\sigma_y^3}e^{-i(\pi/8)\sigma_z^1\sigma_z^2\sigma_z^3}e^{-i(\pi/4)\sigma_x^1}e^{i(\pi/4)\sigma_y^3}, \tag{15}$$

$$e^{i(\pi/8)\sigma_y^1\sigma_z^2\sigma_x^3}=e^{i(\pi/4)\sigma_x^1}e^{-i(\pi/4)\sigma_y^3}e^{i(\pi/8)\sigma_z^1\sigma_z^2\sigma_z^3}e^{-i(\pi/4)\sigma_x^1}e^{i(\pi/4)\sigma_y^3}, \tag{16}$$

$$e^{-i\varphi\sigma_x^1\sigma_x^2}=e^{-i(\pi/4)\sigma_y^1}e^{-i(\pi/4)\sigma_y^2}e^{-i\varphi\sigma_z^1\sigma_z^2}e^{i(\pi/4)\sigma_y^1}e^{i(\pi/4)\sigma_y^2}, \tag{17}$$

$$e^{-i\varphi\sigma_x^2\sigma_x^3}=e^{-i(\pi/4)\sigma_y^2}e^{-i(\pi/4)\sigma_y^3}e^{-i\varphi\sigma_z^2\sigma_z^3}e^{i(\pi/4)\sigma_y^2}e^{i(\pi/4)\sigma_y^3}. \tag{18}$$

Through substituting Eqs. (13)–(18) into Eq. (8) and after simplification, one obtains

$$\begin{aligned}U(t)=&e^{-i(\pi/4)\sigma_y^1}e^{i(\pi/4)\sigma_x^3}e^{-i(\pi/8)\sigma_z^1\sigma_z^2\sigma_z^3}e^{-i(\pi/4)\sigma_y^2}e^{-i\varphi\sigma_z^1\sigma_z^2}\\&\times e^{i(\pi/4)\sigma_y^2}e^{i(\pi/8)\sigma_z^1\sigma_z^2\sigma_z^3}e^{i(\pi/4)(\sigma_x^1+\sigma_x^3)}e^{-i(\pi/4)\sigma_y^3}\\&\times e^{i\frac{\pi}{2}(\sigma_z^1+\sigma_z^3)}e^{-i(\pi/4)\sigma_z^1}e^{-i(\pi/8)\sigma_z^1\sigma_z^2\sigma_z^3}e^{-i(\pi/4)\sigma_y^2}\\&\times e^{-i\varphi\sigma_z^2\sigma_z^3}e^{i(\pi/4)\sigma_y^2}e^{i(\pi/8)\sigma_z^1\sigma_z^2\sigma_z^3}e^{-i(\pi/4)\sigma_x^1}e^{i(\pi/4)\sigma_y^3}.\end{aligned} \tag{19}$$

In Eq. (19), $e^{i(\pi/4)\sigma_y^2}$ is realized by a $\pi/2$ radio frequency (rf) pulse exciting H2 along y axis. Such a pulse is denoted by $[\pi/2]_y^2$. The operation $e^{i(\pi/4)(\sigma_x^1+\sigma_x^3)}$ is realized by a nonselective pulse $[\pi/2]_x^{1,3}$, exciting C1 and C3 simultaneously. The widths of $[\pi/2]_y^2$ and $[\pi/2]_x^{1,3}$ are so short that they can be ignored. The operation $e^{i(\pi/2)(\sigma_z^1+\sigma_z^3)}$ is realized by a pulse sequence

$$[\pi]_x^{1,3}-[\pi]_y^{1,3}, \tag{20}$$

where the time order is from left to right. The operation selective for C1 or C3 can be realized by the established pulse sequence [18,19]. For example, $e^{i(\pi/4)\sigma_x^1}$ is realized by

$$\left[\frac{\pi}{2}\right]_x^1 = \left[\frac{\pi}{2}\right]_y^{1,3} - e^{i(\pi/4)\sigma_z^1} - \left[-\frac{\pi}{2}\right]_y^{1,3}. \tag{21}$$

According to the work of Tseng *et al.* [20], $e^{-i(\pi/8)\sigma_z^1\sigma_z^2\sigma_z^3}$ is realized by

$$\left[-\frac{\pi}{2}\right]_x^2 - [-\pi]_y^2 - \left[\frac{9}{2J_{12}}\right] - \left[\frac{\pi}{2}\right]_y^2 - \left[\frac{1}{4J_{23}}\right] - \left[\frac{\pi}{2}\right]_y^2 - \left[\frac{9}{2J_{12}}\right] - \left[\frac{\pi}{2}\right]_x^2 \tag{22}$$

and $e^{i(\pi/8)\sigma_z^1\sigma_z^2\sigma_z^3}$ is realized by

$$\left[-\frac{\pi}{2}\right]_x^2 - [-\pi]_y^2 - \left[\frac{7}{2J_{12}}\right] - \left[\frac{\pi}{2}\right]_y^2 - \left[\frac{1}{4J_{23}}\right] - \left[\frac{\pi}{2}\right]_y^2 - \left[\frac{7}{2J_{12}}\right] - \left[\frac{\pi}{2}\right]_x^2. \tag{23}$$

The case of only one proton in the sample makes realizing the three-body interactions much easier. One should note that the direct coupling between C1 and C3 is not used.

We choose the state

$$\rho_{iniA} = \sigma_y^1 \tag{24}$$

as the initial state to simulate the *XY* chain in the three-spin system, noting that we use the deviation density matrix to describe the state of the NMR system [21]. The pulse sequence

$$\left[\frac{\pi}{2}\right]_y^2 - \left[\frac{\pi}{2}\right]_y^3 - [\mathrm{grad}]_z - \left[\frac{\pi}{2}\right]_x^1 \tag{25}$$

transforms the system from the equilibrium state

$$\rho_{eq} = \gamma_C(\sigma_z^1 + \sigma_z^3) + \gamma_H\sigma_z^2 \tag{26}$$

to ρ_{iniA} [20], where γ_C and γ_H denote the gyromagnetic ratios of ^{13}C and ^{1}H and $[\mathrm{grad}]_z$ denotes a gradient pulse along the z axis. The irrelative overall factors have been ignored. Using $[U_B, \rho_{iniA}]=0$, we obtain $\rho_A(t)=U(t)\rho_{iniA}U^\dagger(t) = U_A(t)\rho_{iniA}U_A^\dagger(t)$. In experiments, we replace $U(t)$ by $U_A(t)$, in order to shorten the experiment time and simplify the experimental procedure. It is easy to obtain

$$\rho_A(t) = \sigma_y^1\cos^2\varphi + \sigma_z^1\sigma_x^2\frac{1}{\sqrt{2}}\sin(2\varphi) - \sigma_z^1\sigma_z^2\sigma_y^3\sin^2\varphi. \tag{27}$$

When $t=\pi/\sqrt{2}J$, one obtains $\rho_A(\pi/\sqrt{2}J)=-\sigma_z^1\sigma_z^2\sigma_y^3$, which means that the state σ_y has been transferred from C1 to C3. Similarly, if the initial state is chosen as

$$\rho_{iniB} = \sigma_x^1, \tag{28}$$

we obtain

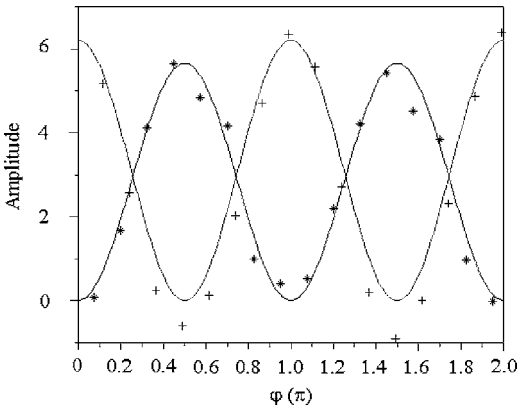

FIG. 2. The graph of the amplitudes of C1 and C3 vs $\varphi = Jt/\sqrt{2}$. The amplitudes have arbitrary units. The data for C1 are marked by "+" and are fitted as $A_1\cos^2\varphi$; the data for C3 are marked by "∗" and are fitted as $A_3\sin^2\varphi$, where $A_1=6.20$ and $A_3=5.65$.

$$\begin{aligned}\rho_B(t) &= U(t)\rho_{iniB}U^\dagger(t)\\ &= U_B(t)\rho_{iniB}U_B^\dagger(t)\\ &= \sigma_x^1\cos^2\varphi - \sigma_z^1\sigma_y^2\frac{1}{\sqrt{2}}\sin(2\varphi) - \sigma_z^1\sigma_z^2\sigma_x^3\sin^2\varphi.\end{aligned} \tag{29}$$

Obviously, $\rho_B(\pi/\sqrt{2}J)=-\sigma_z^1\sigma_z^2\sigma_x^3$, which means that σ_x has been transferred from C1 to C3.

We represent the results of the implementation by NMR spectra. When φ changes, the amplitudes of C1 and C3 change as $\cos^2\varphi$ and $\sin^2\varphi$, respectively. When the initial state is chosen as ρ_{iniA}, the results of implementing $U_A(t)$ are shown in Fig. 2. The data for C1 are marked by "+," and are fitted as $A_1\cos^2\varphi$; the data for C3 are marked by "∗" and are fitted as $A_3\sin^2\varphi$. The two constants $A_1=6.20$ and $A_3=5.65$, with arbitrary units. The experimental results, barring two data for C1, show good agreement with the theoretical expectations. Figure 3 shows the spectra when the state transfers occur. The experimental spectra are listed in the left column, and the simulated spectra without decoherence are listed in the right column for contrast. When $\varphi=0$, $\varphi=\pi/2$, $\varphi=\pi$, $\varphi=3\pi/2$, and $\varphi=2\pi$, the system lies in σ_y^1 (the initial state), $-\sigma_z^1\sigma_z^2\sigma_y^3$, σ_y^1, $-\sigma_z^1\sigma_z^2\sigma_y^3$, and σ_y^1, shown as Figs. 3(a)–3(j), respectively. The experimental results, barring the signals of C1 in Figs. 3(b) and 3(d) the amplitudes of which are shown in Fig. 2, agree with the theoretical expectation quite well. Theoretically, the signals of C1 in Figs. 3(b) and 3(d) should not appear. The time duration for implementing U_A is about 200 ms, which is in the same order with the decoherence time. Hence the decoherence time limit results in the main errors. Moreover, the imperfection of the pulses and the inhomogeneity in the magnetic field also cause errors.

Similar results can be obtained when the initial state is chosen as ρ_{iniB}. Figure 4 shows the implementation of the perfect state transfer when the initial state is ρ_{iniB} and $U(t)$ is replaced by $U_B(t)$. When $\varphi=0$ and $\varphi=\pi/2$, the system lies in

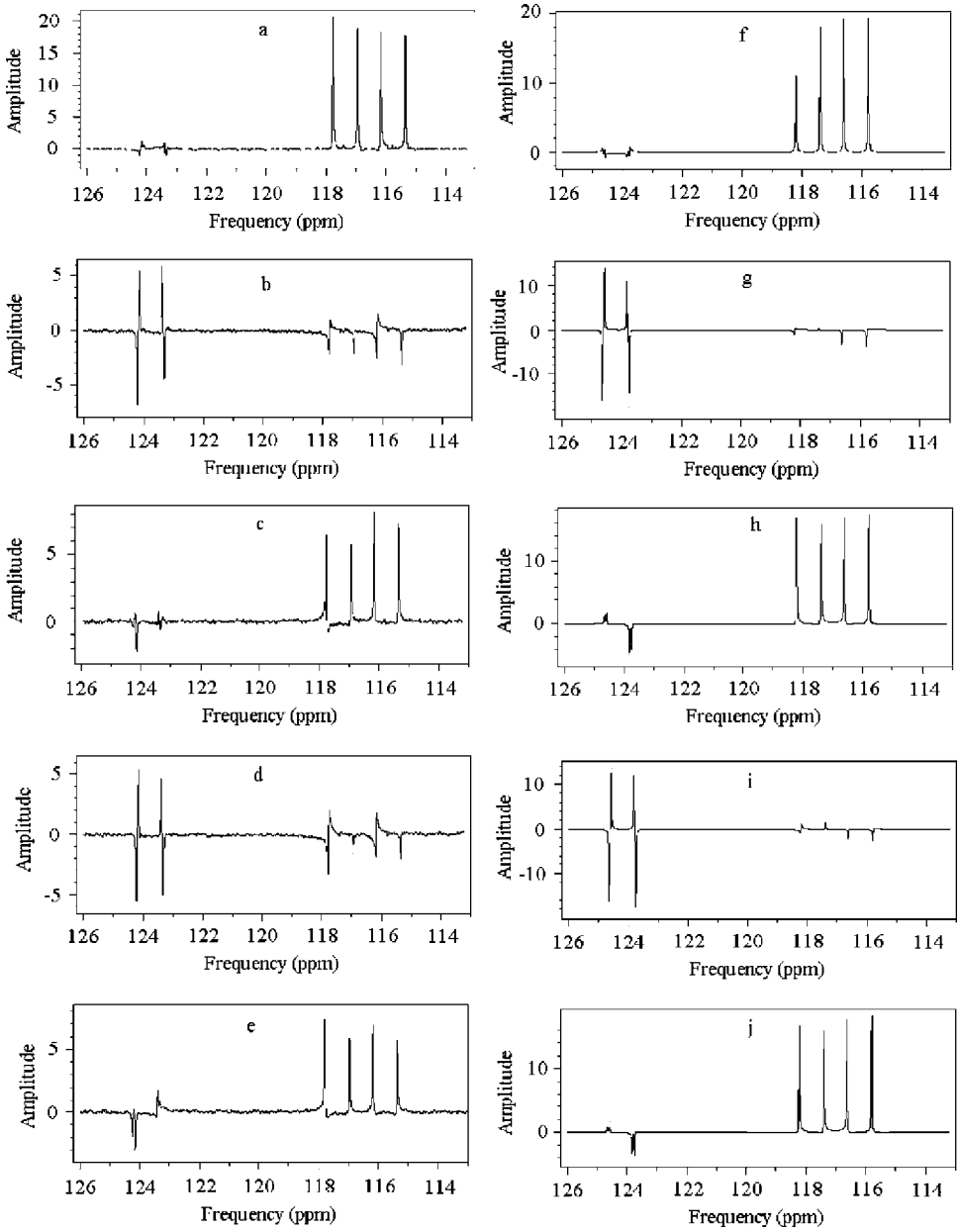

FIG. 3. The carbon NMR spectra of trichloroethylene (TCE) for the implementation of the perfect state transfer when $U_A(t)$ is applied to the initial state σ_y^1. The left column lists the experimental spectra with decoherence, while the right column lists the corresponding simulated spectra without decoherence. When $\varphi=0$, $\varphi=\pi/2$, $\varphi=\pi$, $\varphi=3\pi/2$, and $\varphi=2\pi$, the system lies in σ_y^1 (the initial state), $-\sigma_z^1\sigma_z^2\sigma_y^3$, σ_y^1, $-\sigma_z^1\sigma_z^2\sigma_y^3$, and σ_y^1, shown as (a)–(e) and (f)–(j), respectively. (a) and (f) are the reference spectra used to calibrate the phases of the signals in the two columns, respectively.

σ_x^1 (the initial state) and $-\sigma_z^1\sigma_z^2\sigma_x^3$, shown as Figs. 4(a) and 4(b) for the experimental results and Figs. 4(c) and 4(d) for the simulated results, respectively. We only give the case of $\varphi=\pi/2$, because the other cases require such long time durations that the NMR signals decay seriously due to decoherence. Using Eqs. (7), (12), and (18) and noting that J_{23} is much smaller than J_{12}, one finds that U_B requires a longer time to complete PTS than U_A. For example, when $\varphi=\pi/2$, U_B requires about 300 ms, and when $\varphi=\pi$, U_B requires about 400 ms. When $\varphi=\pi$, $\varphi=3\pi/2$, and $\varphi=2\pi$, we hardly obtain meaningful results due to the limit of the decoherence time.

V. DISCUSSION

We use the amplitudes of NMR signals to define F to describe the qualify for the perfect state transfer. F is defined as

$$F=\frac{I_{PST}}{I_{ini}}. \tag{30}$$

I_{ini} denotes the average amplitude of the quadruple peaks when the system lies in the initial state, and I_{PST} denotes the average amplitude of the desired quadruple peaks after the completion of PST. In Fig. 3, when $\varphi=\pi/2$, $\varphi=\pi$, $\varphi=3\pi/2$, and $\varphi=2\pi$, we obtain $F=30\%$, 34%, 29%, and 34%, respectively, for the experimental results. To explain why the low values of F are mainly caused by decoherence, we give the values of F for the simulated results without decoherence in Fig. 3. They are 77%, 88%, 79%, and 92%, when $\varphi=\pi/2$, $\varphi=\pi$, $\varphi=3\pi/2$, and $\varphi=2\pi$, respectively. In Fig. 4, when $\varphi=\pi/2$, we obtain $F=31\%$ for the experimental result and 82% for the simulated result without decoherence. The simulated results also show that the imperfection of the rf

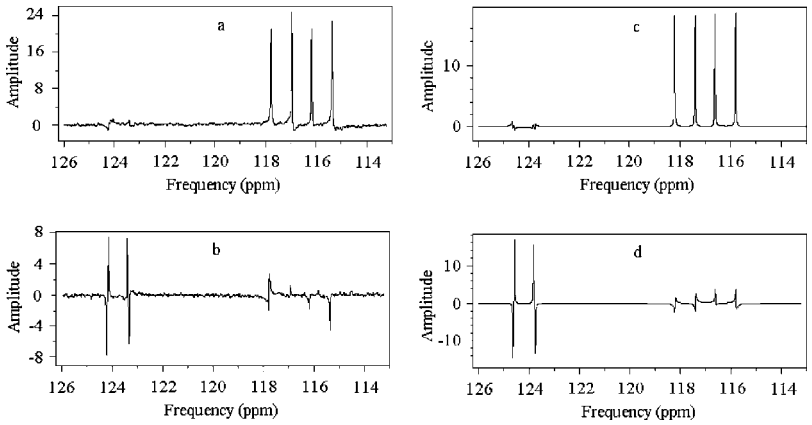

FIG. 4. The carbon NMR spectra of TCE for the implementation of the perfect state transfer when $U_B(t)$ is applied to the initial state σ_x^1. The left column lists the experimental spectra with decoherence, while the right column lists the corresponding simulated spectra without decoherence. When $\varphi=0$ and $\varphi=\pi/2$, the system lies in σ_x^1 (the initial state) and $-\sigma_z^1\sigma_z^2\sigma_x^3$ shown as (a), (b) and (c), (d), respectively. (a) and (c) are the reference spectra. There is a $\pi/2$ phase difference between the reference signals in Figs. 4 and 3.

pulses, especially the shapes of the pulses, is another main source to reduce the fidelity for the PST.

In Figs. 3 and 4, we replace $U(t)$ by $U_A(t)$ and $U_B(t)$ to realize the PST algorithm through choosing two initial states σ_y^1 and σ_x^1, respectively, in order to shorten the experimental time and simplify the experimental procedure. Although the experimental time has been in the same order with T_2, the experimental results are acceptable, except the reduction of the amplitudes of the signals caused by decoherence. If an arbitrary state is chosen as the initial state, the above replacement is invalid. The experiment time to implement the PST is at least 500 ms if the full unitary evolution $U(t)=U_B(t)U_A(t)$ is applied. Such time exceeds T_2, and the effect of decoherence will reduce the quality of PST greatly. Figure 5 represents the experimental result, shown as Fig. 5(b), and the simulated result, shown as Fig. 5(d), when $U(t)$ is applied to the initial state σ_y^1 and $\varphi=\pi/2$. Compared with Fig. 3(b), the signals in Fig. 5(b) are further weakened by decoherence. F for the experimental result is only 11%, while it is 74% for the simulated result. The low value of F shows that meaningful results are hardly obtained if the full $U(t)$ is applied, due to the decoherence time limit of the chemical sample used.

The PST can also be implemented by a series of SWAP operations. For the three-spin chain, the state of spin 1 can be transferred to spin 3 through

$$S_{13}=S_{12}S_{23}S_{12}, \tag{31}$$

where S_{jl} denotes a SWAP operation applying to spins j and l. Just like the discussion in Sec. IV, we also do not use the direct coupling between spins 1 and 3. Using ZZ interactions, one obtains [13]

$$S_{jl}=e^{-i(\pi/4)\sigma_y^j}e^{-i(\pi/4)\sigma_y^l}e^{-i(\pi/4)\sigma_z^j\sigma_z^l}e^{i(\pi/4)\sigma_x^j}e^{i(\pi/4)\sigma_x^l}\times e^{-i(\pi/4)\sigma_z^j\sigma_z^l}e^{i(\pi/4)\sigma_y^j}e^{i(\pi/4)\sigma_y^l}. \tag{32}$$

Through simplification, S_{13} can expressed as

$$\begin{aligned}S_{13}=&e^{-i(\pi/4)(\sigma_y^1+\sigma_y^3)}e^{-i(\pi/4)\sigma_y^2}e^{-i(\pi/4)\sigma_z^1\sigma_z^2}e^{i(\pi/4)\sigma_x^1}e^{i(\pi/4)\sigma_x^2}\\&\times e^{-i(\pi/4)\sigma_z^1\sigma_z^2}e^{-i(\pi/4)\sigma_z^2\sigma_z^3}e^{i(\pi/4)\sigma_x^2}e^{i(\pi/4)\sigma_x^3}e^{-i(\pi/4)\sigma_z^2\sigma_z^3}\\&\times e^{-i(\pi/4)\sigma_z^1\sigma_z^2}e^{i(\pi/4)\sigma_x^1}e^{i(\pi/4)\sigma_x^2}e^{-i(\pi/4)\sigma_z^1\sigma_z^2}\\&\times e^{i(\pi/4)(\sigma_y^1+\sigma_y^3)}e^{i(\pi/4)\sigma_y^2}\end{aligned} \tag{33}$$

and, in matrix form,

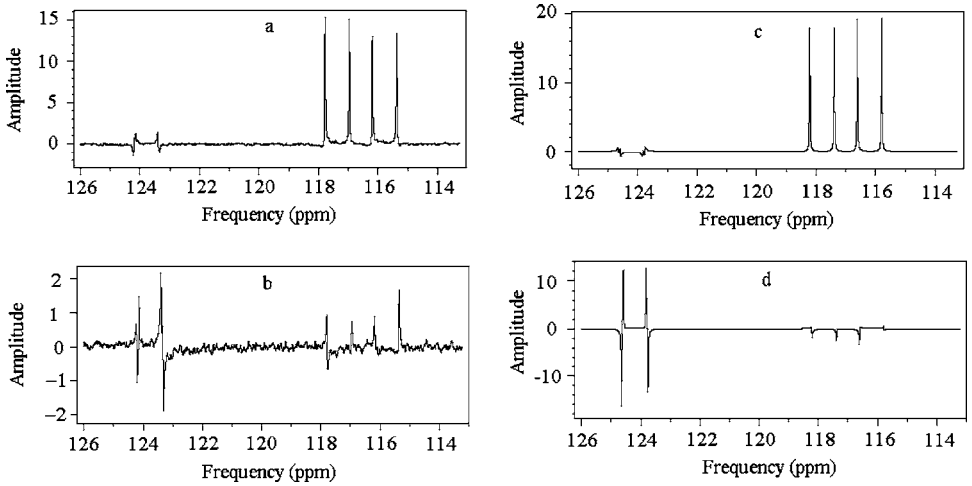

FIG. 5. The carbon NMR spectra of TCE for the implementation of the perfect state transfer when the full unitary evolution $U(t)=U_B(t)U_A(t)$ is applied to the initial state σ_y^1. The left column lists the experimental spectra with decoherence, while the right column lists the corresponding simulated spectra without decoherence. When $\varphi=0$ and $\varphi=\pi/2$, the system lies in σ_y^1 (the initial state) and $-\sigma_z^1\sigma_z^2\sigma_y^3$ shown as (a), (b) and (c), (d), respectively. (a) and (c) are the reference spectra.

$$S_{13} = i \begin{pmatrix} 1 & 0 & 0 & 0 & 0 & 0 & 0 & 0 \\ 0 & 0 & 0 & 0 & 1 & 0 & 0 & 0 \\ 0 & 0 & 1 & 0 & 0 & 0 & 0 & 0 \\ 0 & 0 & 0 & 0 & 0 & 0 & -1 & 0 \\ 0 & 1 & 0 & 0 & 0 & 0 & 0 & 0 \\ 0 & 0 & 0 & 0 & 0 & -1 & 0 & 0 \\ 0 & 0 & 0 & -1 & 0 & 0 & 0 & 0 \\ 0 & 0 & 0 & 0 & 0 & 0 & 0 & -1 \end{pmatrix}. \quad (34)$$

Through comparing Eq. (10) with Eq. (34), one finds that Eq. (10) describes a SWAP operation which is implemented by the *XY* interactions shown as Eq. (1) and can be simulated by Eq. (19) using liquid NMR. Through comparing Eq. (19) with Eq. (33), one finds that Eq. (34) is a bit more easy to realize than Eq. (10) in the liquid NMR system because the *XY* interactions are required to be simulated by rf pulses and *ZZ* interactions. However, in the system where the *XY* interactions really exist, PST through *XY* interactions can be realized much more easily than through SWAP operations.

VI. CONCLUSION

We have simulated a three-spin *XY* chain using liquid NMR. Through defining the proper operators, we use the theories of angular momentum to decompose the evolution caused by *XY* interactions into a series of factors that can be realized by rf pulses and *J* couplings. Such an analog can be helpful for solving the general problems of the Heisenberg chain. As an example for the application of the *XY* chain in quantum computation, the perfect state transfer algorithm is realized in the chain.

We represent the evolution caused by *XY* interactions using a series of single-spin operations and *J* couplings, and hence make it possible to simulate *XY* interactions in the liquid NMR system, although no real *XY* interactions exist there. The simplification of pulse sequence is exploited to shorten the experimental time and to simplify the experimental procedure. In the sample used in our experiments, the coupling constants are not equal to each other. However, we simulate equal couplings in the *XY* chain through choosing the proper evolution time. For perfect state transfer in more than three-spin networks, the coupling strengths are needed to be designed in a proper manner [12]. Our work has shown that such couplings can be well simulated in the liquid NMR system.

ACKNOWLEDGMENTS

This work is supported by the National Natural Science Foundation of China under Grant Nos. 10374010, 60073009, and 10325521, National Fundamental Research Program Grant No. 001CB309308, the Hang-Tian Science Fund, the SRFDP program of Education Ministry of China, and China Postdoctoral Science Foundation. J.-F.Z. is also grateful to Dr. Peng Zhang of the Institute of Theoretical Physics in the Chinese Academy of Science and Professor Jiangfeng Du of the University of Science and Technology of China for their helpful discussions.

[1] A. Steane, Rep. Prog. Phys. **61**, 117 (1998); M. A. Nielsen and I. L. Chuang, *Quantum Computation and Quantum Information* (Cambridge University Press, Cambridge, England, 2000).

[2] R. P. Feynman, Int. J. Theor. Phys. **21**, 467 (1982); S. Lloyd, Nature (London) **273**, 1073 (1996); B. M. Boghosian and W. Taylor IV, Physica D **120**, 30 (1998).

[3] P. W. Shor, in Proceedings of the 35th Annual Symposium on the Foundations of Computer Science, Santa Fe, NM, 1994 (IEEE Computer Society Press, New York 1994).

[4] L. K. Grover, Phys. Rev. Lett. **79**, 325 (1997).

[5] D. Deutsch, Proc. R. Soc. London, Ser. A **400**, 97 (1985); **425**, 73 (1989); D. Deutsch, A. Barenco, and A. Ekert, *ibid.* **449**, 669 (1995); R. Cleve, A. Ekert, C. Macchiavello, and M. Mosca, *ibid.* **454**, 339 (1998); M. J. Bremner, C. M. Dawson, J. L. Dodd, A. Gilchrist, A. W. Harrow, D. Mortimer, M. A. Nielsen, and T. J. Osborne, Phys. Rev. Lett. **89**, 247902 (2002); A. Barenco, C. H. Bennett, R. Cleve, D. P. DiVincenzo, N. Margolus, P. Shor, T. Sleator, J. A. Smolin, and H. Weinfurter, Phys. Rev. A **52**, 3457 (1995).

[6] L. M. K. Vandersypen and I. L. Chuang, Rev. Mod. Phys. **76**, 1037 (2004); D. Loss and D. P. DiVincenzo, Phys. Rev. A **57**, 120 (1998); G. Burkard, D. Loss, and D. P. DiVincenzo, Phys. Rev. B **59**, 2070 (1999); B. E. Kane, Nature (London) **393**, 133 (1998); T. D. Ladd, J. R. Goldman, F. Yamaguchi, Y. Yamamoto, E. Abe, and K. M. Itoh, Phys. Rev. Lett. **89**, 017901 (2002); H. G. Krojanski and D. Suter, *ibid.* **93**, 090501 (2004); R. Vrijen, E. Yablonovitch, K. Wang, H. W. Jiang, A. Balandin, V. Roychowdhury, T. Mor, and D. DiVincenzo, Phys. Rev. A **62**, 012306 (2000); J. I. Cirac and P. Zoller, Phys. Rev. Lett. **74**, 4091 (1995); Nature (London) **404**, 579 (2000); Y. Makhlin, G. Schön, and A. Shnirman, Rev. Mod. Phys. **73**, 357 (2001); M. H. Devoret, A. Wallraff, and J. M. Martinis, e-print cond-mat/0411174; T. Sleator and H. Weinfurter, Phys. Rev. Lett. **74**, 4087 (1995); V. Giovannetti, D. Vitali, P. Tombesi, and A. Ekert, e-print quant-ph/0004107; F. Yamaguchi, P. Milman, M. Brune, J. M. Raimond, and S. Haroche, Phys. Rev. A **66**, 010302(R) (2002); S.-B. Zheng, *ibid.* **70**, 052320 (2004).

[7] L. M. K. Vandersypen, M. Steffen, G. Breyta, C. S. Yannoni, M. H. Sherwood, and I. L. Chuang, Nature (London) **414**, 883 (2001); N. Boulant, L. Viola, E. M. Fortunato, and D. G. Cory, Phys. Rev. Lett. **94**, 130501 (2005); S. Somaroo, C. H. Tseng, T. F. Havel, R. Laflamme, and D. G. Cory, *ibid.* **82**, 5381 (1999); J.-F. Du, T. Durt, P. Zou, H. Li, L. C. Kwek, C. H. Lai, C. H. Oh, and A. Ekert, *ibid.* **94**, 040505 (2005); C. Miquel, J. P. Paz, M. Saraceno, E. Knill, R. Laflamme, and C. Negrevergne, Nature (London) **418**, 59 (2002); X.-H. Peng, J.-F. Du, and D. Suter, Phys. Rev. A **71**, 012307 (2005); C. Negrevergne, R. Somma, G. Ortiz, E. Knill, and R. Laflamme, *ibid.* **71**, 032344 (2005); J.-F. Zhang, G. L. Long, Z.-W. Deng,

W.-Z. Liu, and Z.-H. Lu, *ibid.* **70**, 062322 (2004); X.-D. Yang, A.-M. Wang, F. Xu, and J.-F. Du, e-print quant-ph/0410143.

[8] M. C. Arnesen, S. Bose, and V. Vedral, Phys. Rev. Lett. **87**, 017901 (2001); M. Mohseni and D. A. Lidar, *ibid.* **94**, 040507 (2005); J. P. Keating and F. Mezzadri, *ibid.* **94**, 050501 (2005); L. Zhou, H. S. Song, Y. Q. Guo, and C. Li, Phys. Rev. A **68**, 024301 (2003); S.-J. Gu, H. Li, Y.-Q. Li, and H.-Q. Lin, *ibid.* **70**, 052302 (2004); S.-J. Gu, H.-Q. Lin, and Y.-Q. Li, *ibid.* **68**, 042330 (2003); X.-G. Wang, *ibid.* **66**, 044305 (2002); Phys. Rev. E **69**, 066118 (2004); A. R. Its, B.-Q. Jin, and V. E. Korepin, J. Phys. A **38**, 2975 (2005).

[9] D. Gunlycke, V. M. Kendon, V. Vedral, and S. Bose, Phys. Rev. A **64**, 042302 (2001).

[10] D. P. DiVincenzo, D. Bacon, J. Kempe, G. Burkard, and K. B. Whaley, Nature (London) **408**, 339 (2000).

[11] E. Knill, Nature (London) **434**, 39 (2005); D. Bacon, J. Kempe, D. A. Lidar, and K. B. Whaley, Phys. Rev. Lett. **85**, 1758 (2000).

[12] M. Christandl, N. Datta, A. Ekert, and A. J. Landahl, Phys. Rev. Lett. **92**, 187902 (2004); the extended version: M. Christandl, N. Datta, T. C. Dorlas, A. Ekert, A. Kay, and A. J. Landahl, Phys. Rev. A **71**, 032312 (2005).

[13] Z. L. Madi, R. Brüschweiler, and R. R. Ernst, J. Chem. Phys. **109**, 10603 (1998).

[14] R. R. Ernst, G. Bodenhausen, and A. Wokaum, *Principles of Nuclear Magnetic Resonance in One and Two Dimensions* (Oxford University Press, Oxford, 1987).

[15] D. G. Cory, M. D. Price, and T. F. Havel, Physica D **120**, 82 (1998).

[16] N. Linden, Ē. Kupče, and R. Freeman, Chem. Phys. Lett. **311**, 321 (1999).

[17] J.-F. Du, H. Li, X.-D. Xu, M.-J. Shi, J.-H. Wu, X.-Y. Zhou, and R.-D. Han, Phys. Rev. A **67**, 042316 (2003).

[18] N. Linden, B. Hervè, R. J. Carbajo, and R. Freeman, Chem. Phys. Lett. **305**, 28 (1999).

[19] H. Geen and R. Freeman, J. Magn. Reson. (1969-1992) **93**, 93 (1991).

[20] C. H. Tseng, S. Somaroo, Y. Sharf, E. Knill, R. Laflamme, T. F. Havel, and D. G. Cory, Phys. Rev. A **61**, 012302 (1999).

[21] I. L. Chuang, N. Gershenfeld, M. G. Kubinec, and D. W. Leung, Proc. R. Soc. London, Ser. A **454**, 447 (1998).